PNAS
www.pnas.org

Supplementary Information for

DPYSL3 modulates Mitosis, Migration, and Epithelial-to-Mesenchymal Transition in Claudin-Low Breast Cancer.

Ryoichi Matsunuma, Doug W. Chan, Beom-Jun Kim, Purba Singh, Airi Han, Alexander B. Saltzman, Chonghui Cheng, Jonathan T. Lei, Junkai Wang, Leonardo Roberto da Silva, Ergun Sahin, Mei Leng, Cheng Fan, Charles M. Perou, Anna Malovannaya, Matthew J. Ellis

Matthew J. Ellis
E-mail: matthew.ellis@bcm.edu

This PDF file includes:

Supplementary text
Figs. S1 to S9
Captions for Databases S1 to S3
References for SI reference citations

Other supplementary materials for this manuscript include the following:

Databases S1 to S3

Supporting Information Text

SI Materials and Methods

Antibodies and plasmids

The antibodies used in this study were anti-DPYSL3 antibody (sc-100323, Santa Cruz), anti-DPYSL3 (HPA010948, Sigma Aldrich), anti-p-PAK2 (Ser20) antibody (#2607, Cell Signaling Technology), anti-PAK2 antibody (A301-263A, Bethyl), anti-PAK1 antibody (A301-259A, Bethyl), anti-PAK3 antibody (#1717-1, Epitomics), anti-PAK4 antibody (A300-356A, Bethyl), anti-SNAIL (#3879, Cell Signaling Technology), anti-TWIST (sc-81417, Santa Cruz), anti-Vimentin (sc-73259, Santa Cruz), anti-p-Vimentin (Ser56) (#7391, Cell Signaling Technology), anti-DAPK3 antibody (A304-221A, Bethyl), anti-PKM antibody (sc-365684, Santa Cruz), anti-MARK2 antibody (sc-365405, Santa Cruz), anti-HER2 antibody (MS-730-PABX, Thermo Scientific), anti-Claudin4 antibody (329400, life technologies), anti-Claudin7 antibody (374800, life technologies) and anti-V5 antibody (#46-0705, Invitrogen). DPYSL3-V5 (CRMP4-V5) expression vector and V5 expressed control vector were kindly provided by Dr. Alyson E. Fournier (Montreal Neurological Institute, Montreal, Quebec, Canada) (1). *SNAI1* expression vector, *TWIST1* expression vector and GFP expressed control vector were kindly gifted by Dr. Sendurai A. Mani (MD Anderson Cancer Center, Houston, TX) (2).

RNA interference

Luciferase shRNA plasmids, and shRNA bacterial stocks of DPYSL3 were purchased from Santa Cruz (SHC007, TRCN0000046848 and TRCN0000418591). shDPYSL3_1 sequence was 5′-CCGGCCAAACGGTTGTGATCTAAAGC TCGAGCTTTAGATCACA-ACCGTTTGGTTTTTTG-3′. The sequence for shDPYSL3_2 was 5′- CCGATAACTCCTTCATG GTTTATATCTCGAGATAT-AAACCATGAAGGAGTTATTTTTTG-3′. Lentivirus was packaged by co-transfection of constructs with the MISSION Lentiviral Packaging Mix (Sigma Aldrich) and Fu gene HD (Roche) into 10 cm plates HEK293T cells. Medium was changed after 24 hours, and 48 hours supernatants were pooled and filtered through a 0.45 μm filter. WHIM12 and Hs578T were transduced with each construct and selected on 0.5 μg/ml puromycin. The siRNA sequence used to target DPYSL3 was 5′-GGAAGAAUAUCUGUGGGUUtt-3′, and siRNA oligonucleotides targeting PAK1 and PAK2, and siRNA as a negative control were purchased from Sigma-Aldrich (SASI_Hs02_00334074, SASI_Hs01_00014672 and SIC001).

RNA extraction and quantitative real-time PCR (qRT-PCR)

Total RNA was extracted from each cell line and tumor using RNeasy Mini Kit (QIAGEN, Venlo, Netherlands) according to the manufacturer's protocol. RNA was reverse transcribed into cDNA using iScript cDNA Synthesis Kit (Bio-Rad, California, USA) in a 20 μL reaction according to the manufacturer's protocol. Equal amounts of cDNA were used as templates for qRT-PCR to detect the level of each mRNA expression relative to that of *GAPDH* (endogenous control). mRNA expression was quantitated using an LightCycler96 (Roche, IN, USA) and SYBR Green qPCR SuperMix (Invitrogen, Carlsbad, CA, USA). For *DPYSL3*, the forward and reverse primers were *DPYSL3*-F 5′-AGCTCTATGAGATCTTCACC-3′ and *DPYSL3*-R 5′-ATGATATCCCCATTCTCAGC-3′, respectively; for *SNAI1*, the forward and reverse primers were *SNAI1*-F 5′-TCGGAAGCCTAACTACAGCGA -3′, *SNAI1*-R 5′-AGATGAGCATTGGCAGCGAG-3′, respectively; for *DPYSL3* short isoform (CRMP4a), the forward and reverse primers were *DPYSL3* short isoform (CRMP4a)-F 5′-CATTCACTCCACCTGATCTC-3′ and *DPYSL3* short isoform (CRMP4a)-R 5′-CCCTCCTTCTTCTGCTCC-3′, respectively; for *DPYSL3* long isoform (CRMP4b), the forward and reverse primers were *DPYSL3* long isoform (CRMP4b)-F 5′-GAAGACGATCTGCCCGTGTA-3′, *DPYSL3* long isoform (CRMP4b)-R 5′-AAATCCAGCGTCTTGCTCTC-3′, respectivelyfor *GAPDH*, the forward and reverse primers were *GAPDH*-F 5′-CCTGGATACCGCAGCTAGGA-3CHAR13 and *GAPDH*-R 5′-GCGGCGCAATACGAATGCCCC-3′, respectively. qRTPCR reactions were performed in triplicate. Fold induction of gene expression was calculated using the $2^{-\triangle\triangle CT}$ method.

Immunoprecipitation and Western Blotting

The lysates were incubated with specific antibodies (sc-100323 was used for DPYSL3 antibody, Santa Cruz) under constant rotation. Protein A or G beads were added 1 hour later and incubated for an additional 30 minutes, followed by extensive washing [20 mM HEPES (pH 7.6), 150 mM KCl, 1 mM Dithiothreitol, 0.1 % NP40, and 8 % glycerol supplemented with protease and phosphatase inhibitors]. The protein A or G beads were boiled in 2× Laemmli buffer, and the precipitated proteins were separated by SDS-PAGE. The proteins were transferred onto nitrocellulose membranes, and Western blotting was performed and analyzed with specific antibodies (HPA010948 was used for DPYSL3 antibody, Sigma Aldrich) as described (3).

Immunofluorescence analysis

Cells were briefly washed in extraction buffer (Microtubule Stabilization Buffer (MTSB): 100 mM PIPES pH 6.8, 1 mM EGTA, 5 mM MgCl2), incubated with MTSB/0.05 % Triton X- 100 for 2 minutes at room temperature, and fixed with 2 % paraformaldehyde (PFA) /0.02 % Triton X-100 in MTSB for 1 hour at room temperature. Cells were blocked in 5 % BSA/0.2 % Triton X-100 in PBS for 30 minutes at room temperature. Primary antibodies (β–tubulin, 1:100) and phalloidin (1:1000) diluted in 0.5 % BSA in PBS were incubated for 3 hours at room temperature. Secondary antibodies were diluted in 0.5 % BSA in PBS for 1 hour at room temperature. Actin was visualized with an Alexa Fluor 488 phalloidin (ab176753, Abcam).

Cover slips were mounted using ProLong® Diamond Antifade Mountant (Thermo Scientific) and images were acquired with a Nikon Eclipse Ti-E. β-tubulin was used to distinguish between mitosis and multiple nucleation. The number of nuclei per cell in more than 10 random fields of stained cells was manually counted. For vimentin staining, anti-Vimentin antibody as a primary antibody was diluted with 1:200.

Immunohistochemistry

IHC staining was performed with assistance from The Lester and Sue Smith Breast Center Pathology Core at Baylor College of Medicine (Houston, TX, USA). Tissue sections were incubated at 58ºC overnight in a dry slide incubator and deparaffinized in xylene and graded alcohol washes. Antigen retrieval was performed in 0.1 M Tris-HCl pH 9.0 following by quenching in 3 % H2O2. Ki67 (clone MIB-1, Dako, 1:200) antibody, CD44 (Thermo Fisher Scientific, MS-668-P1) and CD24 (Thermo Fisher Scientific, MS-1279-P) were used to stain for 1h at RT. After washing in TBS, EnVision labelled polymer-HRP anti-mouse antibody (Dako) was added for 30 min. at RT. Slides were washed with TBS then developed with DAB+ solution (Dako) and DAB sparkle enhancer (Biocare). After washing in TBS, slides were counterstained with Hematoxylin, dehydrated, and cleared before coverslipping with Cytoseal (VWR).

Mitotic spread analysis

Cells were treated with 0.1 μg/ml Colcemid™ for 6 h. After hypotonic lysis of 75 mM KCl for 40 min, cells were fixed for 30 min in a fixing solution of methanol: acetic acid (3:1). Metaphase spreads were produced on glass slides and chromosomes were stained with propidium iodide (PI). After images were captured chromosome numbers were counted.

Cell cycle analysis

2×10^5 cells were plated in 6-well plates. After trypsinization and collection, cells were washed with 2 % FBS in PBS and fixed in 70 % ethanol overnight at -20 °C. Cells were then washed with 2 % FBS in PBS. Cells were incubated with RNase A (DNase free) and PI for 30 min at 37°C. The percentages of cells in different phases of the cell cycle were measured with an Accuri C6 (Accuri Cytometers) flow cytometer.

Alamarblue growth assay

1000 cells/well were plated into 96 well cell culture plates. Cell growth was quantified by Alamarblue assay at Day 1, Day 3, and Day 5, (or Day 7) post plating and relative growth was calculated as Day X/Day 1 ratios.

Transwell migration assay

WHIM12 shLuc and shDPYSL3 cell migration were quantified by transwell assays using uncoated (8 μm pore size; Costar, Corning Inc Cambridge, Cat No. 3422) in 24-well plates. Briefly, cells were trypsinized and seeded onto the upper chamber of the transwells (1×10^5 cells/well) in supplement-free Ham's F-12 medium. The lower chamber of the transwells was filled with Ham's F-12 medium containing supplement with collagen1 40 μg/ml. The chambers were incubated at 37°C with 5 % CO2 for 3.5 hr. At the end of incubation, cells on the upper surface of the filter were removed using a cotton swab. Cells migrating through the filter to the lower surface were fixed with 70 % ethanol for 10 min and stained with 1 % crystal violet for 20 min. Cells were photographed at 10× magnification, and three fields each from triplicate samples were counted to quantify migration.

Invasion assay

WHIM12 shLuc and shDPYSL3 cell migration were quantified by transwell assays using uncoated (8 μm pore size; Costar, Corning Inc Cambridge, Cat No. 3422) in 24-well plates. 70 μl of Matrigel was plated onto the well and incubated for 1 hr before cells were trypsinized and seeded onto the upper chamber of the transwells (5×10^4 cells/well) in supplement-free Ham's F-12 medium. The lower chamber of the transwells was filled with Ham's F-12 medium containing supplement. The chambers were incubated at 37°C with 5 % CO2 for 48 hr. At the end of incubation, cells migrating through the filter to the lower surface were fixed with 70 % ethanol for 15 min, then cells on the upper surface of the filter were removed using a cotton swab and stained with 0.5 % crystal violet for 30 min. After 250 μl of 33 % acetic acid was added to the lower chamber to elute dye, 100 μl of elute was transfer to 96-well plates and optical density was measured.

Statistical analyses

Student's t test and ANOVA followed by Tukey's or Bonferroni's post-hoc test were performed using GraphPad Prism® statistical software (GraphPad Soft- ware Inc., San Diego, CA, USA). $p<0.05$ was considered statistically significant. In some analyses, Student's t test was performed with Microsoft® Excel.

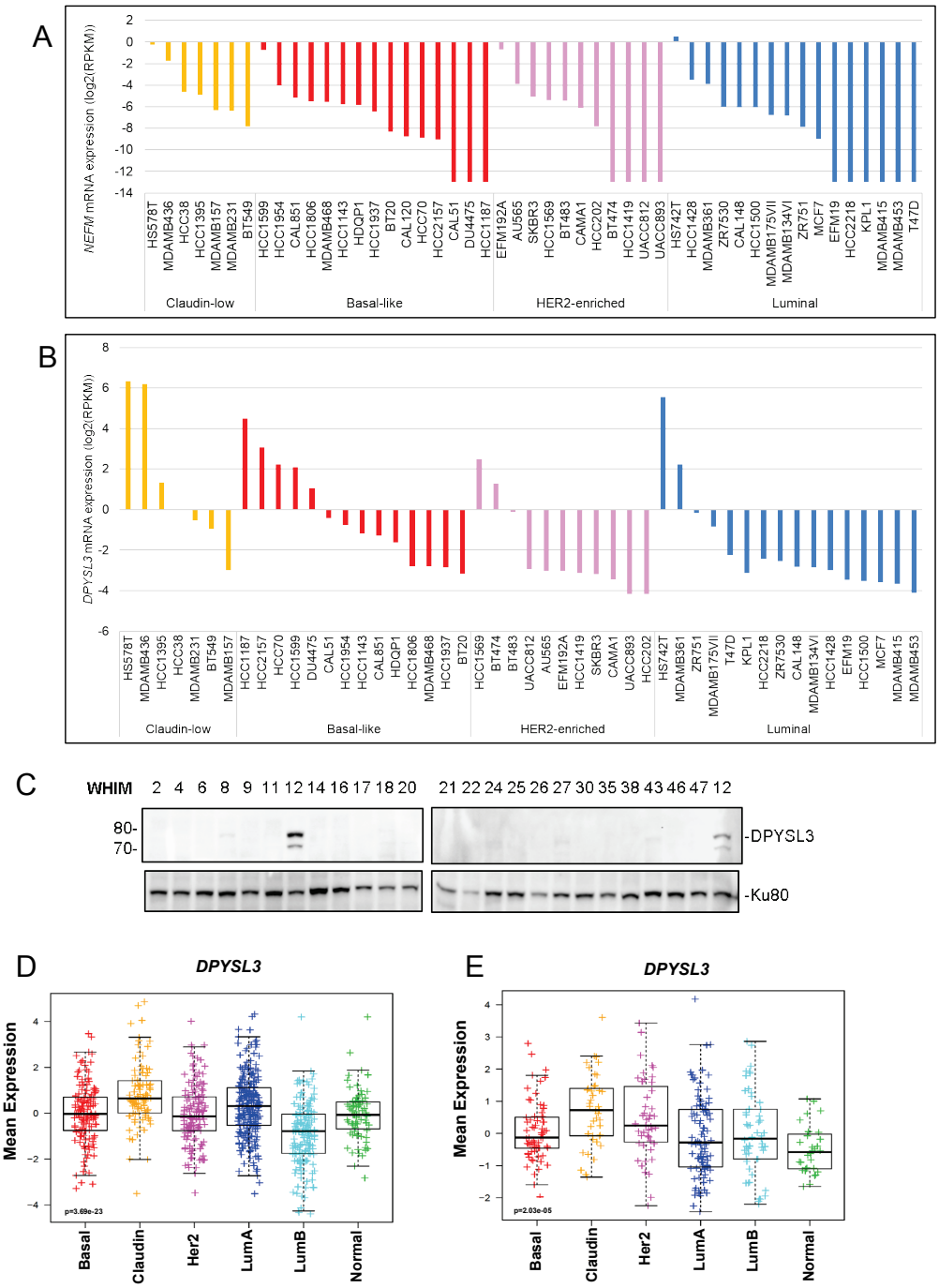

Fig. S1. DPYSL3 is highly expressed in CLOW breast cancer. (A) mRNA expression data of *NEFM* across breast cancer cell lines of various intrinsic subtypes from Broad Institute Cancer Cell Line Encyclopedia (CCLE) (4). RPKM (Reads per kilobase per million mapped reads) is a normalization method which is widely used in RNA-Sequencing and represents gene expression levels. (B) mRNA expression data of *DPYSL3* across breast cancer cell lines of various intrinsic subtypes from Broad Institute Cancer Cell Line Encyclopedia (CCLE) (4). RPKM (Reads per kilobase per million mapped reads) is a normalization method which is widely used in RNA-Sequencing and represents gene expression levels. (C) Western blotting for DPYSL3 expression across 24 WHIM PDX tumors of various intrinsic subtypes. WHIM12 is the only CLOW PDX. Ku80 used as a loading control. (D) (E) Box and whiskers plots with center line representing mean mRNA expression levels of *DPYSL3* gene expression across intrinsic subtypes from breast tumor datasets; Harrell's dataset (D) (5) and UNC dataset (E) (6). Box extends to inter-quartile range (IQR) and whiskers extend to 1.5 × IQR of mean gene expression. basal-like (Basal), claudin-low (Claudin), HER2-enriched (Her2), luminal A (LumA), luminal B (LumB) and normal-like (Normal). p-value determined by Kruskal-Wallis test.

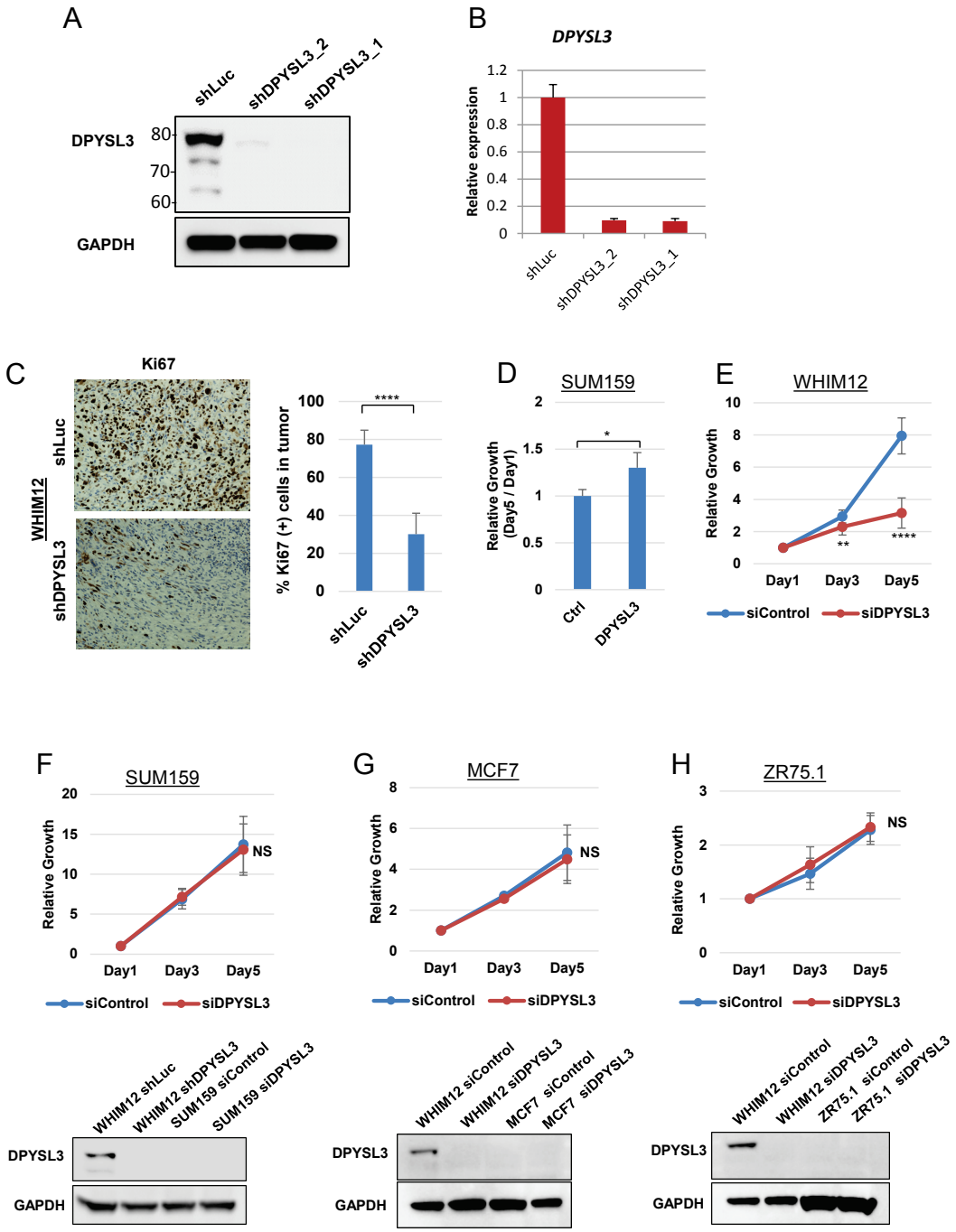

Fig. S2. Loss of DPYSL3 suppresses proliferation. (A) Western blotting for DPYSL3 levels in stable WHIM12 shLuc, shDPYSL3_1 and shDPYSL3_2 cell lines. (B) *DPYSL3* transcript levels as measured by mRNA-qPCR in stable WHIM12 shLuc, shDPYSL3_1, and shDPYSL3_2 cell lines. Expression normalized to shLuc. (C) (Left panel) Representative IHC images of Ki67 expression WHIM12 xenograft tumor sections. More than 5,000 cancer cells from each group were counted and then the percentage of Ki67 positive cells were evaluated. (Right panel) Quantification showing averages counts from 4 tumor sections from each group ±SD. p-value was calculated with student's t test (**** $p < 0.0001$). (D) Growth of SUM159 cells transfected with control vector (Ctrl) or DPYSL3 expression vector (DPYSL3). Data are averages from three independent experiments ±SEM. p-value was calculated with student's t test (* $p < 0.05$). (E)(F)(G)(H) Growth of indicated cell lines transfected with siControl or siDPYSL3. Data are averages from three independent experiments ±SEM (** $p < 0.01$; **** $p < 0.001$, student's t-test) (upper panels). Bottom panels show western blots to compare DPYSL3 expression levels.

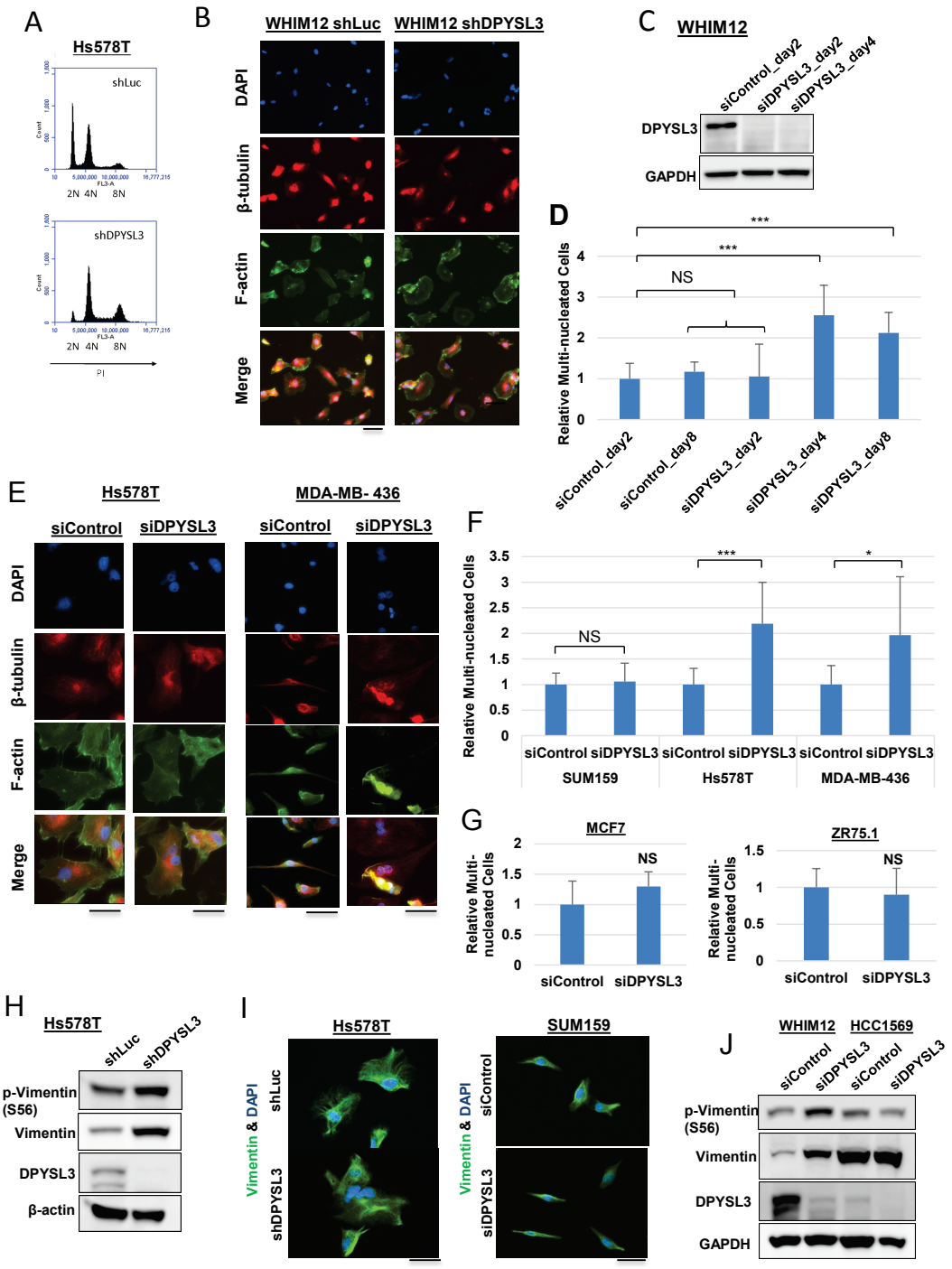

Fig. S3. Loss of DPYSL3 induces multiple nucleation in CLOW breast cancer. (A) Histogram depicting cell cycle distributions of stable Hs578T shLuc and shDPYSL3 cells by flow cytometry stained with PI. (B) Representative IF images of stable WHIM12 shLuc and shDPYSL3_1 cells stained with phalloidin, β-tubulin and DAPI. β-tubulin was used to distinguish between mitosis and multiple nucleation. (C) Western blotting showing DPYSL3 in lysates of WHIM12 siControl and WHIM12 siDPYSL3 cells on day 2 and day 4 after transfection. (D) Bar graphs depicting average number of mutli-nucleated cells from immunofluorescence was performed after transient transfection of siControl or siDPYSL3 in WHIM12 cells ±SEM from three independent experiments. p-value determined by ANOVA (Tukey's multiple comparisons test). (E)(F) Representative IF images of siControl or siDPYSL3 transfected Hs578T cells and MDA-MB 436 cells (E). β-tubulin was used to distinguish between mitosis and multiple nucleation. Quantification of multi-nucleated cells relative to siControl transfected indicated cells with statistical significance determined by student's t test (F). (G) 4 days post-transfected MCF7 and ZR75.1 with siControl and siDPYSL3 cells were stained with phalloidin, β-tubulin and DAPI for immunofluorescence to examine multi-nucleation. The number of nuclei per cell in more than 10 random fields of stained siControl and siDPYSL3 cells was manually counted. p-value was from student's t test. (H) Western blotting was performed with the indicated antibodies in Hs578T shLuc and shDPYSL3 cells. (I) Representative IF images of stable Hs578T shLuc and shDPYSL3 cells and 4 days post-transfected SUM159 cells with siControl and siDPYSL3 were stained with vimentin (pseudo-colored in green) and DAPI (pseudo-colored in blue). (J) Western blotting of p-Vimentin, Vimentin, and DPYSL3 in WHIM12 and HCC1569 cells transfected with siControl or siDPYSL3.

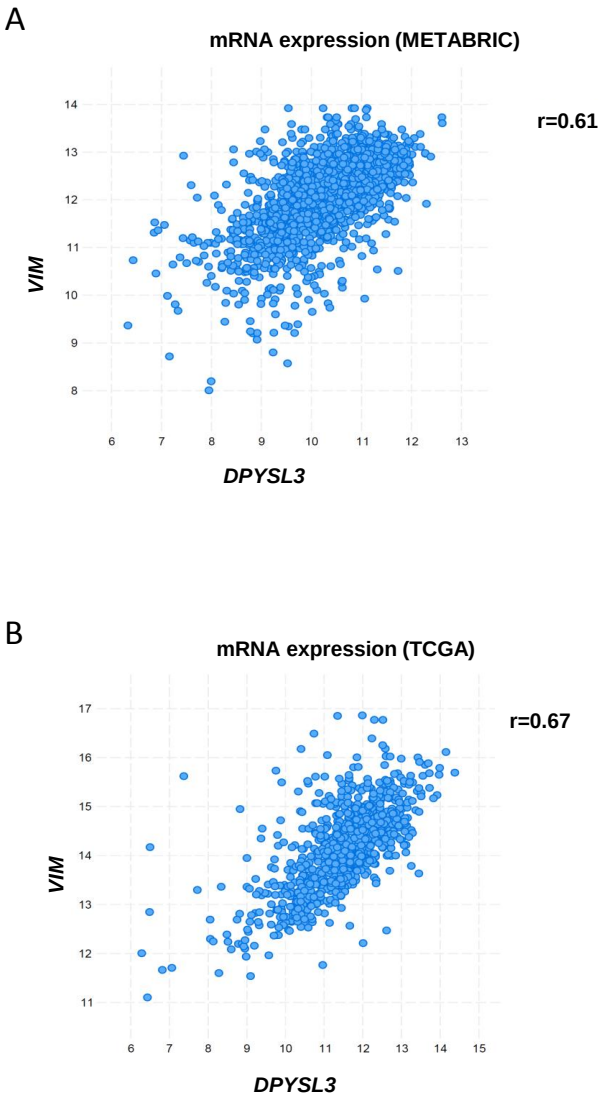

Fig. S4. Correlation between mRNA expression levels of *VIM* and *DPYSL3*. (A) Correlation data of 1904 breast samples from the METABRIC dataset (7)(8). Pearson's r = 0.61. (B) Correlation data of 817 breast samples from the TCGA dataset (9). Pearson's r = 0.67.

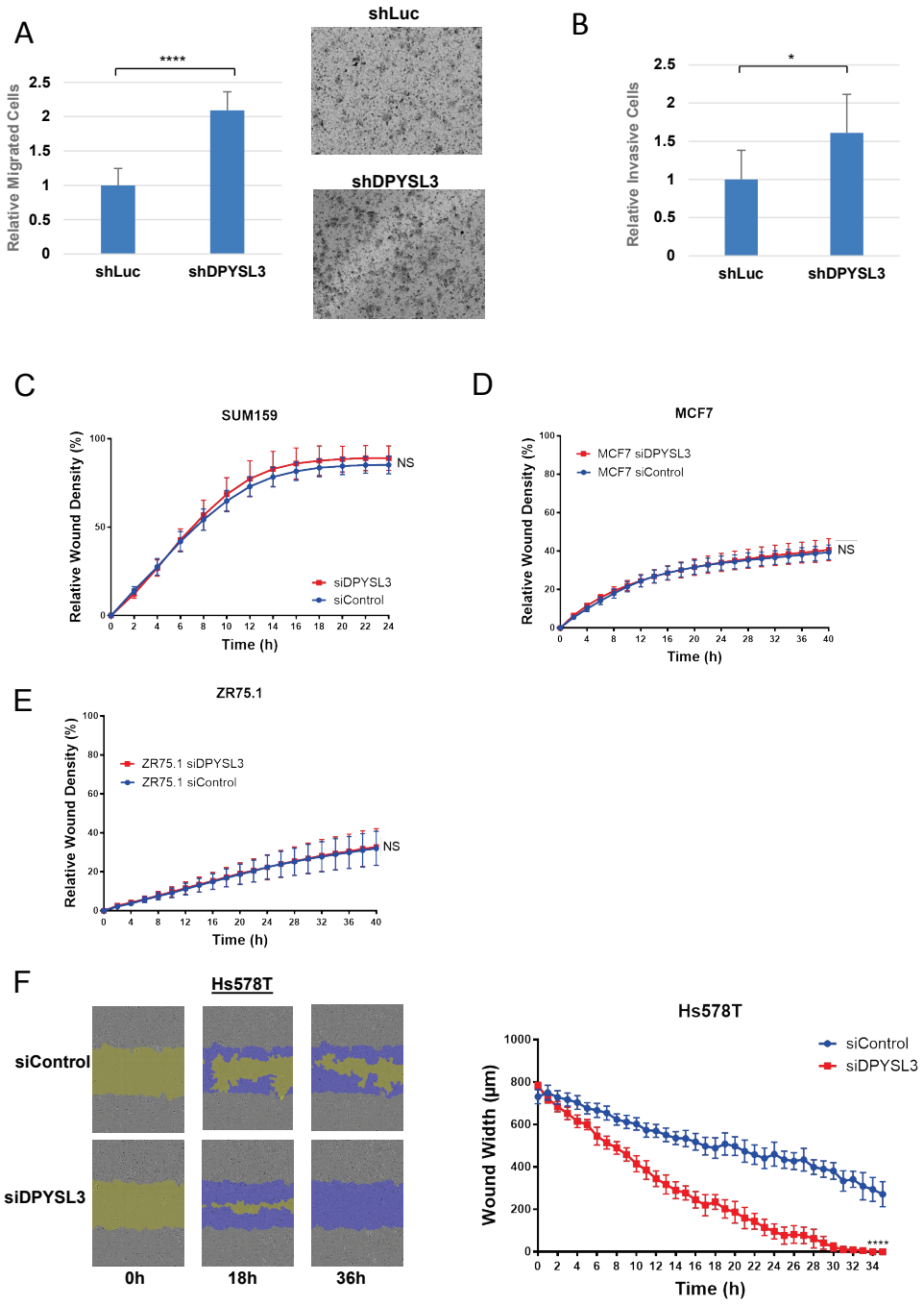

Fig. S5. DPYSL3 inhibits migration in CLOW breast cancer. (A) (Left panel) Bar graphs depicting average number of migrated cells from stable WHIM12 shLuc and shDPYSL3 cells with representative images of crystal violet stained cells shown in the right panel. Data are averages from three independent experiments ±SEM (**** $p < 0.001$, student's t-test). (B) Bar graphs depicting quantification of cell invasion from stable WHIM12 shLuc and shDPYSL3 cells. Data are averages from three independent experiments ±SEM (* $p < 0.05$, student's t-test). (C)(D)(E) Quantification of cell migration from scratch wound healing assay of SUM159 (C), MCF7 (D) and ZR75.1 (E) transfected with siControl or siDPYSL3 in the presence of mitomycin C proliferation blocking agent. Data are averages from three independent experiments ±SEM. (F) (Left panel) Representative cell migration images from scratch wound healing assay at indicated times post wounding of Hs578T cells transfected with siControl or siDPYSL3. Yellow region denotes wound area post wounding. Migrated cells into the wound area are pseudo-colored blue to aid visualization. (Right panel) Quantification of wound width during course of experiment. p-value was calculated with student's t test (**** $p < 0.0001$).

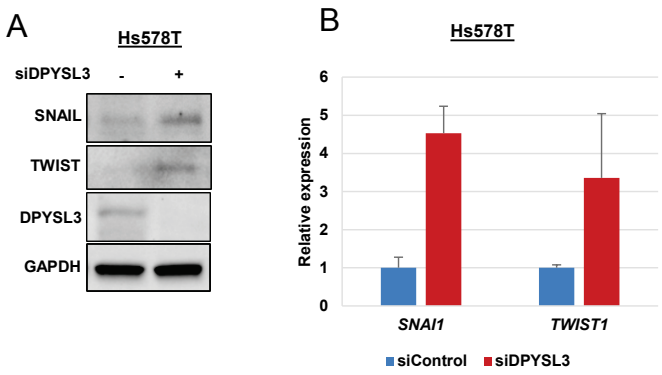

Fig. S6. DPYSL3 regulates EMT markers in CLOW breast cancers. (A) Western blotting of SNAIL, TWIST, and DPYSL3 in Hs578T cells transfected with siControl or siDPYSL3. GAPDH used as a loading control. (B) *SNAI1* and *TWIST1* transcript levels measured by mRNA-qPCR in Hs578T cells transfected with siControl or siDPYSL3. Results are presented in-terms of a fold change relative to siControl.

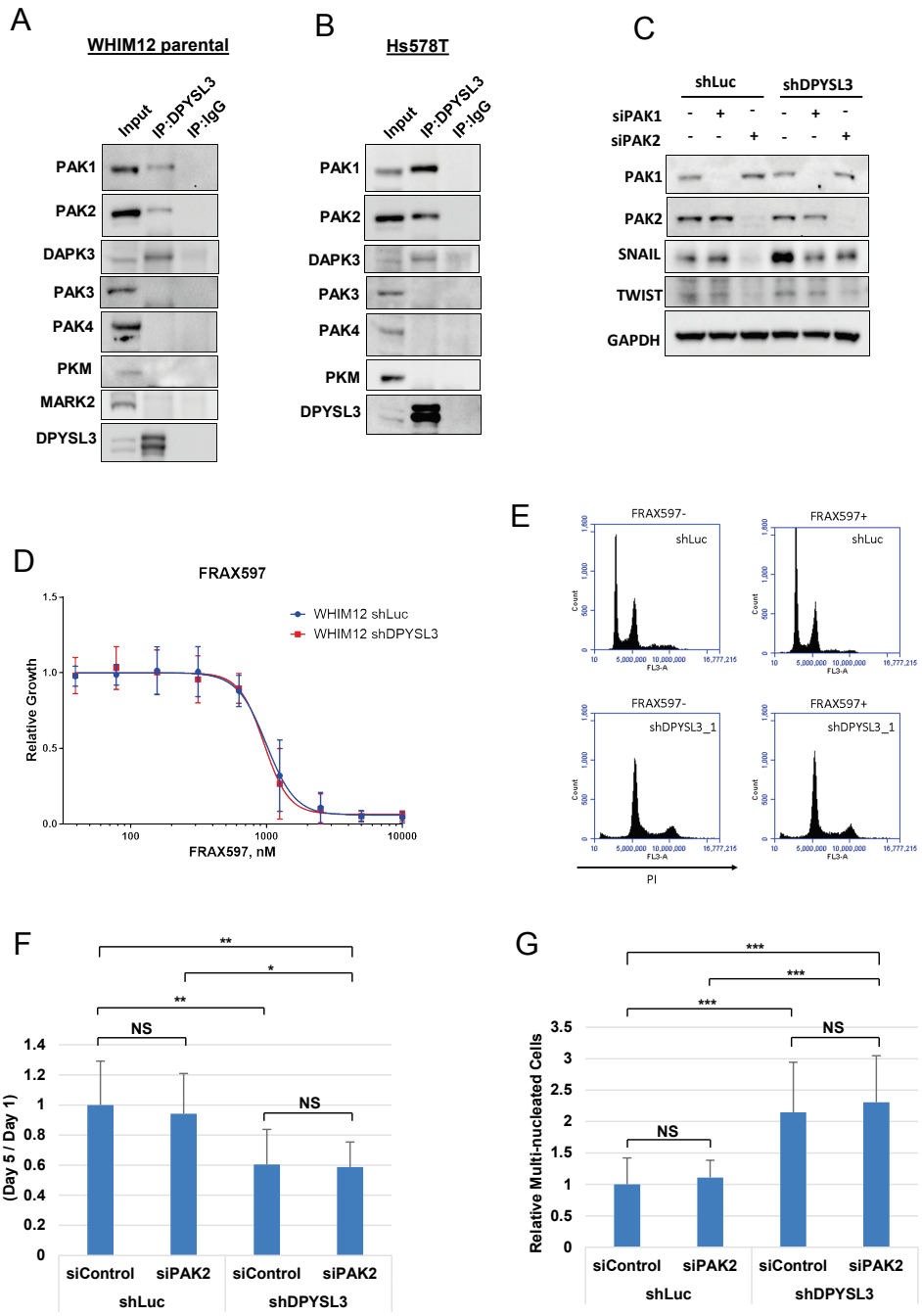

Fig. S7. PAK2 is dispensable for mitosis and proliferation in CLOW breast cancers. (A)(B) Immunoprecipitation with DPYSL3 was tested for interaction with indicated antibodies in WHIM12 cells (A) and Hs578T cells (B). IgG IP was used as a negative control. (C) Western blotting showing PAK1, PAK2, SNAIL, and TWIST in lysates of siControl, siPAK1 and siPAK2 4-day post transfected WHIM12 cells. (D) Dose response curve assessing cell viability (Alamar blue assay) in WHIM12 shLuc and WHIM12 shDPYSL3 cells after treatment with FRAX597. Data are averages ±SEM from three independent experiments. (E) Flow cytometric cell cycle histograms of WHIM12 shLuc and WHIM12 shDPYSL3_1 cells stained with PI after 2.5 μM of FRAX597 treatment for 24h. (F) Growth of WHIM12 shLuc and shDPYSL3 cells transfected with siControl or siPAK2. Data are averages from three independent experiments ±SEM (* $p < 0.05$; ** $p < 0.01$, ANOVA with Tukey's multiple comparisons test). (G) WHIM12 shLuc and shDPYSL3 cells were transfected with siRNA of control or PAK2. Cells were stained with phalloidin, β-tubulin and DAPI for immunofluorescence to study microtubule formation 4 days after the transfection. The number of nuclei per cell in more than 10 random fields of each cells was manually counted. p-value was from ANOVA (Tukey's multiple comparison test).

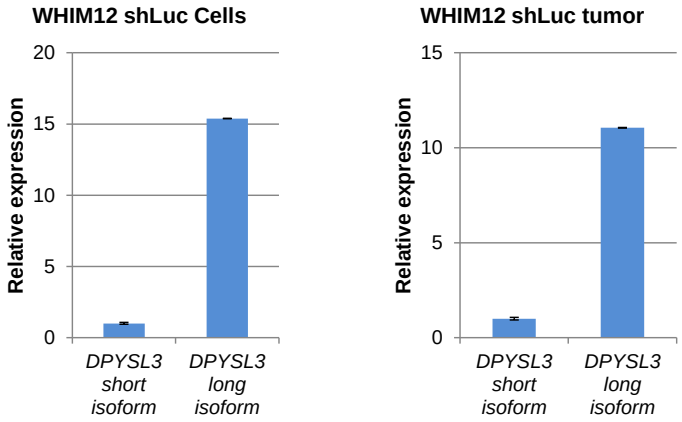

Fig. S8. Bar graphs depicting expression of *DPYSL3* isoforms in WHIM12 shLuc cells (left panel) and WHIM12 shLuc xenograft tumors (right panel) analyzed by qRT-PCR.

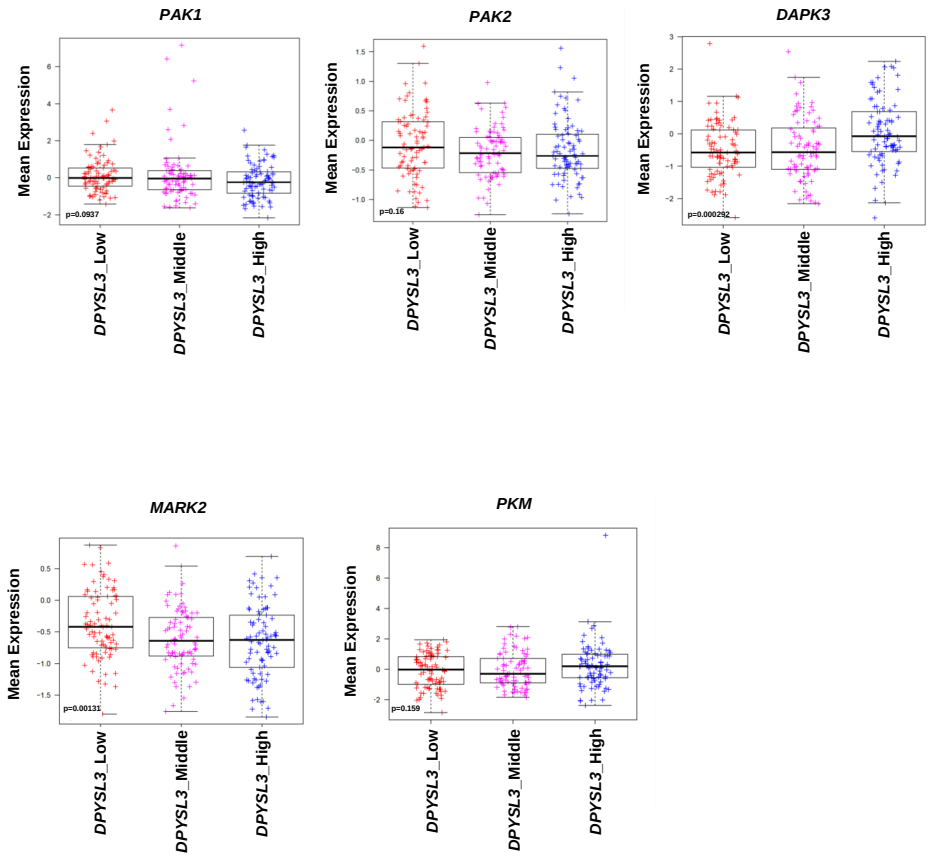

Fig. S9. Box and whiskers plots with center line representing mean mRNA expression levels of *PAK1/2*, *DAPK3*, *MARK2* and *PKM* of CLOW tumors in METABRIC dataset (7)(8). Box extends to inter-quartile range (IQR) and whiskers extend to 1.5 × IQR of mean gene expression. Comparison of gene expression signatures among three ranks (Low, Middle, or High) of *DPYSL3* expression. p-value determined by Kruskal-Wallis test.

Additional data table S1 (dataset_S1.txt)

ANOVA results across each subtype for each DataSource (phospho, profiling, and RNAseq), including the F statistic (F), degrees of freedom (df), pValue, BH-FDR adjusted value (qValue), claudin-low log2 fold change (WHIM12), Entrez GeneID, gene observation counts and data sources each gene is observed (DataCounts and Sources) and GeneSymbol.

Additional data table S2 (dataset_S2.txt)

Overlap of average claudin-low gene expression values across (Expression) with number of PubMed citations (Total) and after filtering by "Claudin low" and "breast cancer" keywords (filtered).

Additional data table S3 (dataset_S3.txt)

Immunoprecipitation and Mass Spectrometry analysis. After incubation with anti-DPYSL3 antibody, DPYSL3 complex was pulled down from WHIM12 shLuc and WHIM12 shDPYSL3 lysate.

References

1. Alabed YZ, Pool M, Tone SO, Fournier AE (2007) Identification of crmp4 as a convergent regulator of axon outgrowth inhibition. *Journal of Neuroscience* 27(7):1702–1711.
2. Bollong MJ, et al. (2017) A vimentin binding small molecule leads to mitotic disruption in mesenchymal cancers. *Proceedings of the National Academy of Sciences* p. 201716009.
3. Chan DW, Ting NS, Lees-Miller SP, Mody CH (1996) Purification and characterization of the double-stranded dna-activated protein kinase, dna-pk, from human placenta. *Biochemistry and cell biology* 74(1):67–73.
4. Barretina J, et al. (2012) The cancer cell line encyclopedia enables predictive modelling of anticancer drug sensitivity. *Nature* 483(7391):603.
5. Harrell JC, et al. (2012) Genomic analysis identifies unique signatures predictive of brain, lung, and liver relapse. *Breast cancer research and treatment* 132(2):523–535.
6. Prat A, et al. (2010) Phenotypic and molecular characterization of the claudin-low intrinsic subtype of breast cancer. *Breast cancer research* 12(5):R68.
7. Curtis C, et al. (2012) The genomic and transcriptomic architecture of 2,000 breast tumours reveals novel subgroups. *Nature* 486(7403):346.
8. Pereira B, et al. (2016) The somatic mutation profiles of 2,433 breast cancers refine their genomic and transcriptomic landscapes. *Nature communications* 7:11479.
9. Ciriello G, et al. (2015) Comprehensive molecular portraits of invasive lobular breast cancer. *Cell* 163(2):506–519.